ELSEVIER

International Journal of Adhesion & Adhesives 21 (2001) 137–144

International Journal of Adhesion & Adhesives

Evaluation of the cure kinetics of the wood/pMDI bondline

David P. Harper[a], Michael P. Wolcott[a,*], Timothy G. Rials[b]

[a]Department of Civil and Environmental Engineering, Washington State University, Pullman, WA 99164-1806, USA
[b]USDA Forest Service, Southern Research Station, Pineville, LA 71360, USA

Accepted 25 October 2000

Abstract

Micro-dielectric analysis (μDEA) and differential scanning calorimetry (DSC) were used to monitor cure of polymeric diphenylmethane diisocyanate (pMDI) resin with wood strands in a saturated steam environment. A first-order autocatalyzed kinetic model was employed to determine kinetic parameters. The kinetics were found to follow an Arrhenius relation. A single ramp DSC technique and μDEA produced models that predicted similar results at higher cure temperatures, but the μDEA-based model predicts a longer cure time at low temperatures. The isothermal μDEA method yields higher activation energies and Arrhenius frequency factors than models based on single DSC ramps. A modification to ASTM E698 was made to conform to the assumption of autocatalyzed kinetics. The modified ASTM E698 method predicted an earlier end of cure than the μDEA-based models and was in agreement with DSC results obtained by partial cure experiments. The activation energies and frequency factors for the different cure monitoring methods are sensitive to different stages of cure. © 2001 Elsevier Science Ltd. All rights reserved.

Keywords: B. Wood; Polymeric isocyanate; Cure kinetics; Dielectric analysis

1. Introduction

When producing wood composites, the primary manufacturing objective is to minimize the time to develop adequate mechanical strength for resisting delamination upon opening the press. However, the wood/adhesive system is exposed to rapidly changing conditions of pressure, steam, and heat during manufacture. The pMDI reacts with the water vapor upon exposure. The early part of cure is dominated by chain extension of pMDI prepolymers and little is contributed to strength development [1]. The latter stages of cure are dominated by the development of a polymer network. During the development of the three-dimensional network adhesive strength also develops. The cure of the pMDI adhesive in this system is a separate issue than the nature of the adhesive bond. However, the bond and cure are related and simultaneously occurring processes. Kinetic modeling is one means that can be used to optimize the cure process.

Controversy abounds over the exact nature of the cure of polymeric diphenylmethane diisocyanate (pMDI) on wood substrates produced under realistic processing environments [2–6]. The possible reaction products include polyurea, biuret/polyuret, allophanate, and polyurethane bonds. The complex nature of the reaction makes mechanistic approaches to modeling extremely difficult and favors phenomenological methods. However, phenomenological methods are only accurate if the test conditions used to generate the kinetic data are realistic to those in manufacturing.

Few methods used to evaluate cure can be applied in realistic processing environments [7–9]. For pMDI-bonded wood composites the primary challenge is to contain and evaluate the cure in a steam environment that is produced in hot-pressed panels. Differential scanning calorimeter (DSC) and micro-dielectric analysis (μDEA) are two methods where volatile gases can be contained during cure evaluation. A saturated environment can be created inside the DSC pan, but mechanical pressure cannot be applied to the sample as in manufacturing. Numerous studies have been conducted using calorimetric techniques to evaluate resin cure [3,10,11]. It has been shown that the cure of pMDI in a saturated steam environment can be monitored in situ using μDEA [1]. The change in dielectric signal can then be applied to a phenomenological model of cure:

$$\frac{d\alpha}{dt} = kf(\alpha). \tag{1}$$

* Corresponding author. Tel.: + 1-509-335-2262; fax: + 1-509-335-5077.

0143-7496/01/$ - see front matter © 2001 Elsevier Science Ltd. All rights reserved.
PII: S0143-7496(00)00045-2

A basic rate equation (Eq. (1)) relates the rate of cure at a constant temperature to a function ($f(\alpha)$) of cure by a constant (k), where α is the degree of cure.

The rate constant follows the Arrhenius equation

$$\ln k = \ln A - \frac{E}{RT}, \tag{2}$$

where E is the activation energy, A is the Arrhenius frequency factor, R is the ideal gas constant, and T is the temperature. The Arrhenius frequency factor relates the amount of collisions that need to occur in a unit time to carry out the reaction, and the activation energy describes the amount of energy needed to propagate cure.

Two types of phenomenological kinetic models available for modeling thermosetting adhesives are nth order and autocatalyzed [12]. The thermoset models are related to the rate equation by $f(\alpha)$. Reactions that have their greatest rate of cure at the onset of the reaction are characterized as nth order. For $f(\alpha)$ an nth-order reaction is described by Eq. (3), where n is the order of the reaction.

$$f(\alpha) = (1 - \alpha)^n \tag{3}$$

In contrast, autocatalyzed kinetics is characterized by $d\alpha/dt$ reaching a maximum at 30–40% cure [12]. In general, autocatalyzed reactions take the following form:

$$\frac{d\alpha}{dt} = k\alpha^m(1 - \alpha)^n, \tag{4}$$

where m and n sum to equal the overall reaction order. Most commonly, a maximum rate of cure is reached at 45–55% of cure. Although this behavior does not strictly follow the specified criteria, it certainly is more accurate than an nth-order kinetics approach. Standardized methods exist for evaluating kinetic parameters of nth-order reactions (ASTM E698-79 1979). However, these methods must be modified for autocatalyzed models [12–14].

2. Objectives

The overall objective in modeling the cure process of pMDI is to optimize processing parameters to shorten pressing cycles. To optimize a process using pMDI adhesives, two events must be considered in the model: (1) the point at which the bond strength can resist panel delamination and (2) reduction of free isocyanate levels for safe storage. The important association between the chemical and mechanical properties in modeling can be illustrated where both conditions must be satisfied. In this case, a phenomenological approach that encompasses the overall process may be more useful than a mechanistic model that may not accurately relate to mechanical property development. To achieve this overall goal the specific objectives are:

1. Analytically model the cure of pMDI in a saturated steam environment.
2. Employ the use of μDEA in evaluating cure for model development.
3. Utilize an autocatalyzed model employing only one rate constant.
4. Compare single and multiple ramp calorimetric methods of modeling.
5. Relate the kinetic models to physical phenomenon.

3. Methods and materials

Aspen (*Populus tremuloides*) flakes were obtained and prepared for μDEA [1]. A commercially available pMDI was sprayed on the aspen flakes at 3,5, or 7% levels (oven dry mass basis). The flake-pair assemblies were pressed at isothermal temperatures of 110, 120, 130, and 140°C in the presence of saturated steam. μDEA was performed by a Micromet Eumetric System III dielectric analyzer with an IDEX senson in order to observe the change in conductivity while flake pairs were pressed in an enclosed steam-producing press [1]. A criterion was established for the onset and end of cure. The onset of cure was taken as the maximum conductivity, σ_{max}, and the end was taken as the absolute minimum value of the slope to obtain an overall change in conductivity, $\Delta\sigma$. The minimum value for the slope was calculated by numerically taking the derivative of the log $\sigma(t)$ curve with respect to time. Where, the end of cure occurs when the slope is 0.01 log(siemens)s^{-1}. The degree of cure at a time, t, can then be calculated by:

$$\alpha(t) = \frac{\log \sigma_{max} - \log \sigma(t)}{\log \Delta\sigma}. \tag{5}$$

In preparation for DSC analysis, pMDI was applied to two aspen flakes at a 7% level. A 25-mg sample was removed with a small hole punch from the flake pair. For analysis, the sample was placed in a hermetically sealed, stainless-steel DSC pan with 2 μl of distilled water to provide enough moisture to create a saturated steam environment. The samples were analyzed in the DSC while they were heated from 30 to 200°C at heating rates (β) of 1, 5, 10, 15, and 20°C/min. A fresh specimen was used for each DSC ramp. The exothermic heat generation was then measured for each ramp. The degree of cure was calculated from the exotherm as

$$\alpha = \frac{Q(t)}{Q_0}, \tag{6}$$

where $Q(t)$ is the residual heat at time, t and Q_0 is the total heat of reaction. Q_0 was calculated by numerically integrating the power spectra with respect to time using the trapezoidal method.

Partial cure DSC experiments and lap-shear experiments were prepared simultaneously in an enclosed steam-producing press [1]. The samples were pressed at a specified temperature and time to obtain 0–100% cure as determined by dielectric analysis. A 25-mg sample was then removed from a flake pair and prepared as discussed above for DSC. A ramp of 20°C/min was performed and the exothermic heat measured. The α was then calculated as the ratio of heat generation of a partially cured sample to that of an uncured sample at the same heating rate. Lap-shear specimens were pulled in tension on a universal testing machine at a rate of 1.27 mm/min until failure. Failures were noted as adhesive, cohesive, or wood failures.

An autocatalyzed kinetics model (Eq. (4)) was used for both isothermal and ramp curing studies. The collected data were used as input into the model to estimate kinetic parameters in the Arrhenius relationship. By integrating Eq. (1) comparisons were made between parameters and results previously obtained for pMDI cure [1].

4. Results and discussion

4.1. Micro-dielectric analysis

A model of autocatalyzed kinetics was used to determine kinetic parameters of the μDEA results. Starting with the model for autocatalyzed kinetics in Eq. (4), a linear expression may be obtained. Assuming a first-order reaction where $m + n = 1$, the equation can be rearranged and expressed as

$$\ln\left(\frac{\mathrm{d}\alpha/\mathrm{d}t}{\alpha}\right) = \ln k + n\ln\left(\frac{1-\alpha}{\alpha}\right). \tag{7}$$

This form can now be used to determine k and n. The relationship of k to the cure temperature can be used to determine Arrhenius parameters. As an alternative to this method, the Arrhenius relation can be substituted directly into Eq. (7) to yield

$$\ln\left(\frac{\mathrm{d}\alpha/\mathrm{d}t}{\alpha}\right) = \ln A - \frac{E}{RT} + n\ln\left(\frac{1-\alpha}{\alpha}\right). \tag{8}$$

Eq. (8) can then be fit to the calculated cure with multiple linear regression. Because the reaction order of $m + n = 1$ was assumed in this derivation, an alternative method for determining reaction orders is by finding the maximum rate of cure. Take the derivative of Eq. (4) with respect to (t), yielding the second derivative of α with respect to time, and evaluate at $\alpha = \alpha_{max}$, where α_{max} is the degree of cure at the maximum rate of cure,

$$\alpha_{max} = m. \tag{9}$$

Comparisons to second-order kinetics can be made by substituting $m + n = 2$. Such a comparison is used to validate the use of first-order kinetics over higher orders. Thus Eq. (8) will be changed to

$$\ln\left(\frac{\mathrm{d}\alpha/\mathrm{d}t}{\alpha^2}\right) = \ln k + n\ln\left(\frac{1-\alpha}{\alpha}\right). \tag{10}$$

This will also influence the reaction order where

$$\alpha_{max} = \frac{m}{2}. \tag{11}$$

This result for second-order kinetics was achieved by Lam [14].

Linear regressions were performed to compare first- and second-order kinetics (Figs. 1 and 2). A higher coefficient of determination (R^2) was achieved for the first-order model than second order. Only the linear portion of the data was fit to a linear regression to determine rate constants and reaction orders. Near the end of cure the reaction becomes diffusion controlled, which is not accurately represented in this model. The values for n and m were observed to be dependent on temperature (Fig. 3). The overall reaction order does not change, but m and n do affect the rates of conversion (Eq. (4)), which may have an impact on ramp cure studies.

A linear regression was performed to calculate the Arrhenius parameters (Fig. 4 and Table 1). Integrating Eq. (1) (Fig. 5) can facilitate a comparison between the predicted and experimental results for cure. Although the predicted results are close to what is experimentally observed, the model predicts an earlier end of cure then what is experimentally observed. Further, the model is not sensitive to the resin load for the selected resin levels. The experimentally observed differences in resin loads arise late in cure where diffusion control likely occurs [1].

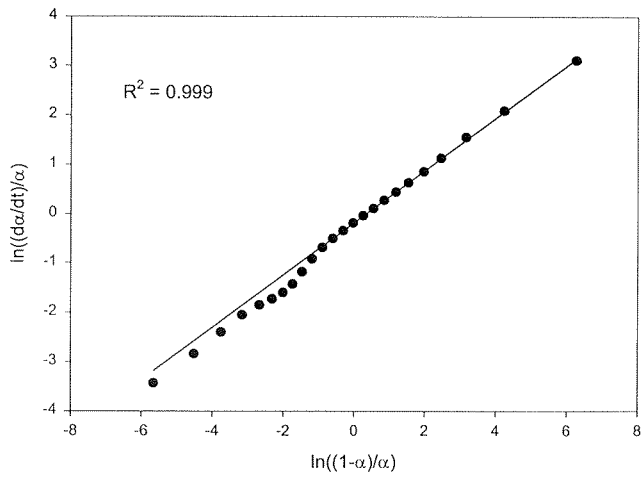

Fig. 1. First-order kinetic plot for 120°C isotherm and 5% pMDI with linear regression for data obtained by μDEA.

4.2. Multiple ramps

The ASTM E698-79 method is a very accurate and effective method for evaluating the kinetics of thermally unstable systems [12,15]. Kinetic parameters can be estimated from multiple ramps with different heating rates. For ASTM E698-79, a first-order kinetic model is fit to the exothermic temperature peak (T_p) in the DSC data. The basis for this model is that the peak occurs at a constant cure, α_{max}, and that an nth-order reaction is followed [14]. Both assumptions are often violated by autocatalyzed reactions. The violations are illustrated by the temperature dependence of α_{max} that was observed for the ramps (Table 2). Therefore, the ASTM method was modified to fit autocatalyzed kinetics. Starting with first-order kinetics and Eq. (4), and considering the maximum degree of cure (α_{max}) occurring at time (t_{max}),

$$f(\alpha_{max}) = \int_0^{\alpha_{max}} \frac{d\alpha}{\alpha^{1-n}(1-\alpha)^n} = \int_0^{t_{max}} A e^{-E/RT} dt. \quad (12)$$

Using a constant heating rate ($\beta = dT/dt$),

$$f(\alpha_{max}) = \int_0^{\alpha_{max}} \frac{d\alpha}{\alpha^{1-n}(1-\alpha)^n} \approx \int_0^{T_p} \frac{A}{\beta} e^{-E/RT} dT. \quad (13)$$

The right-hand integral can be solved considering a substitution for $u = E/RT$ and $u_0 = E/RT_p$,

$$f(\alpha_{max}) \approx \frac{AE}{\beta R}\left(\frac{\exp(-u_0)}{u_0} - \int_{u_0}^{\infty} \frac{\exp(-u)}{u} du\right), \quad (14)$$

$$p(u) = \left(\frac{\exp(-u_0)}{u_0} - \int_{u_0}^{\infty} \frac{\exp(-u)}{u} du\right). \quad (15)$$

Values for $p(u)$ have been tabulated and for its linear interpolation [16]. Prime [12] utilized Doyle's solution to obtain a linear form for $60 \geqslant \mu_0 \geqslant 20$:

$$\ln\beta + f(\alpha_{max}) \approx \ln\left(\frac{AE}{R}\right) - 5.33 - \frac{1.05E}{RT_p}. \quad (16)$$

The Arrhenius parameters can be solved by plotting $\ln\beta + \ln f(\alpha_{max})$vs.$1/T_p$. By following the ASTM method for predicting activation energies, similar results to the modified method can be obtained. Since the ASTM method neglects the slight dependence of α_{max} on temperature, a modification to A is necessary. Prime [12] has previously modified A to fit autocatalyzed kinetics,

$$A \cong \frac{\beta E e^{E/RT_p}}{RT_p^2[2\alpha_{max} + 2B\alpha_{max} - 3\alpha_{max}^2 - B]}, \quad (17)$$

where B is a stoichiometric ratio of reactants. $B = 1$ is

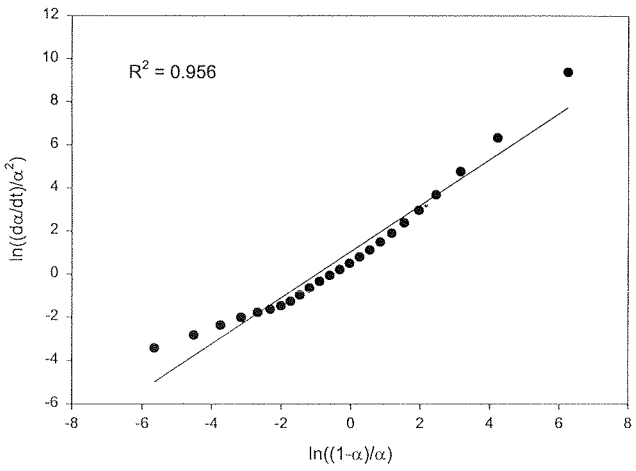

Fig. 2. Second-order kinetic plot for 120°C platens and 5% pMDI with linear regression for data obtained by μDEA.

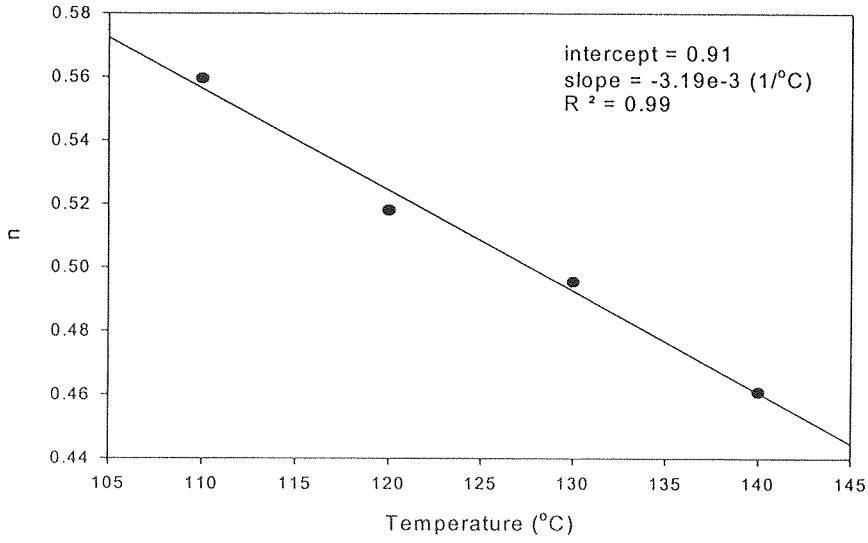

Fig. 3. Temperature dependence of n, the reaction order, from μDEA isotherms.

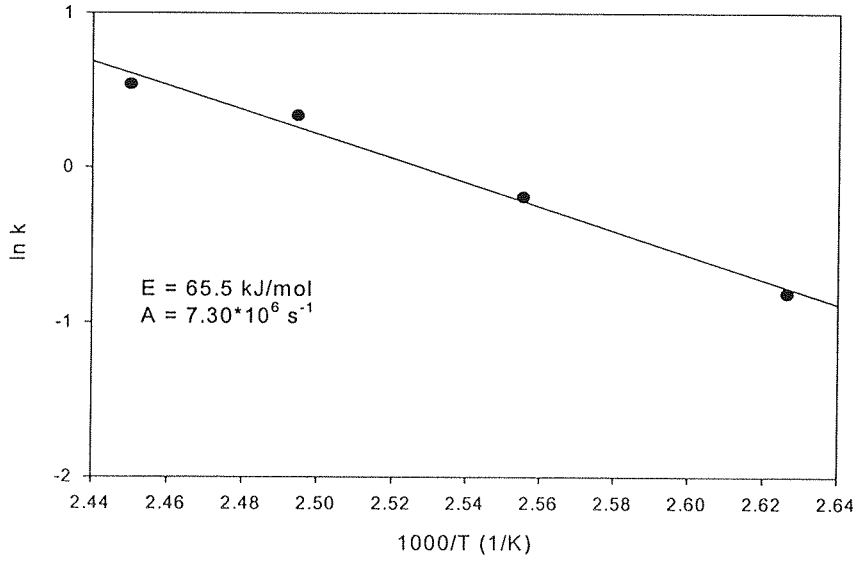

Fig. 4. Determination of Arrhenius parameters from the plot of $\ln k$ versus $1000/T$ for 5% pMDI by μDEA isotherms.

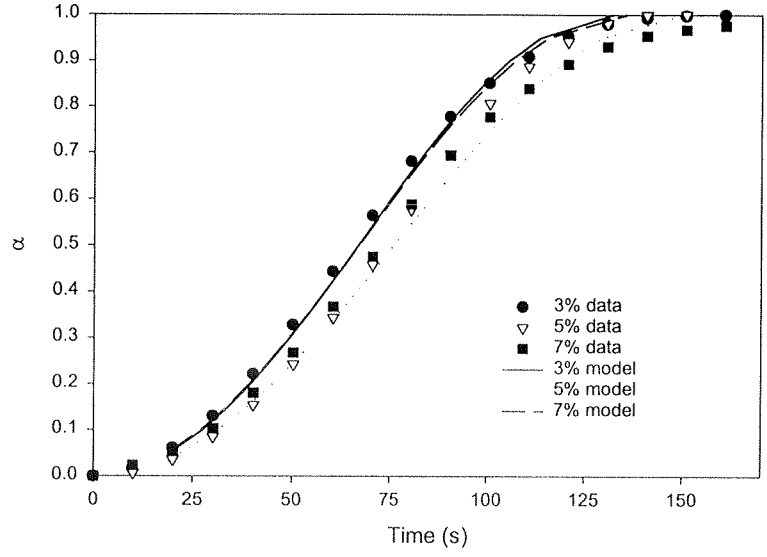

Fig. 5. Comparison of data and model generated from kinetic parameters determined from μDEA for 130°C.

Table 1
Arrhenius parameters obtained by μDEA isotherms at varying weight percents of pMDI on an oven-dried wood basis

Percent pMDI	E (kJ/mol)	$A \times 10^5 (s^{-1})$
3	75.1	1500
5	65.5	73
7	82.6	3550

Table 2
DSC ramps results for temperature, degree of cure, and the peak exotherm

β(°C/min)	T(°C)	α_{max}(%)	$f(\alpha_{max})$
1	79.6	71.8	1.99
5	105.4	68.9	1.93
10	118.8	68.3	1.91
15	126.3	67.1	1.89
20	134.0	67.3	1.89

assumed when the quantities of reactants are mixed. Results from the modified ASTM and modified A methods $E = 62.1$ kJ/mol and $A = 4.28 \times 10^6$ and $E = 60.1$ kJ/mol and $A = 1.927 \times 10^6 s^{-1}$, respectively.

These results produce similar results for predicting cure (Fig. 6). The multiple ramps compare favorably with results previously obtained for end of cure by partial cure studies [1].

4.3. Single temperature ramp

Kinetic parameters can be obtained by considering only a single temperature ramp at a specified heating rate. Starting with Eq. (4) and the Arrhenius equation, kinetic parameters can be estimated from a single temperature ramp:

$$k = \frac{(\mathrm{d}\alpha/\mathrm{d}t)}{\alpha^m(1-\alpha)^n} = A\mathrm{e}^{-E/RT}. \tag{18}$$

Parameters calculated from a nonlinear regression showed similar results for each ramp (Table 3). The nonlinear regressions were performed for up to 80% of cure. The parameters obtained from the individual ramps produce similar results for all temperatures with the exception of 1°C/min temperature ramps.

4.4. Physical interpretation of models

Cure was predicted for isothermal conditions by numerically integrating Eq. (4). The results obtained from the multiple ramp cure models and those from partial cure studies display agreement at isothermal temperatures above 120°C (Fig. 6). The multiple ramp methods utilize the maximum point on the DSC spectrum only, and the partial cure study was conducted by observing the heat generated during cure as a whole. Because most of early heat generation prior to the maximum is likely isocyanate consumption contributing to increases in the molecular weight of the polymer, the exothermic peak does not represent structures or reaction products that form late in cure. The divergence between the model and experimental results for low-temperature cure are likely to come from suspected morphological differences between pMDI cured at low and high temperatures [1]. The single ramp DSC techniques tend to disagree with the partial cure experiments. However, the single ramp technique comes close to predicting the partial cure of the 110°C isotherm and agrees more closely with μDEA results.

Table 3
Kinetic parameters obtained from DSC ramp methods

Method/β(°C/min)	E (kJ/mol)	$A \times 10^5$(s^{-1})	n
Modified ASTM	62.1	42.8	0.31
Modified *A*	60.1	23.2	0.31
1	61.3	24.2	0.52
5	55.3	4.00	0.51
10	55.5	3.88	0.50
15	55.5	3.96	0.49
20	55.5	4.08	0.51

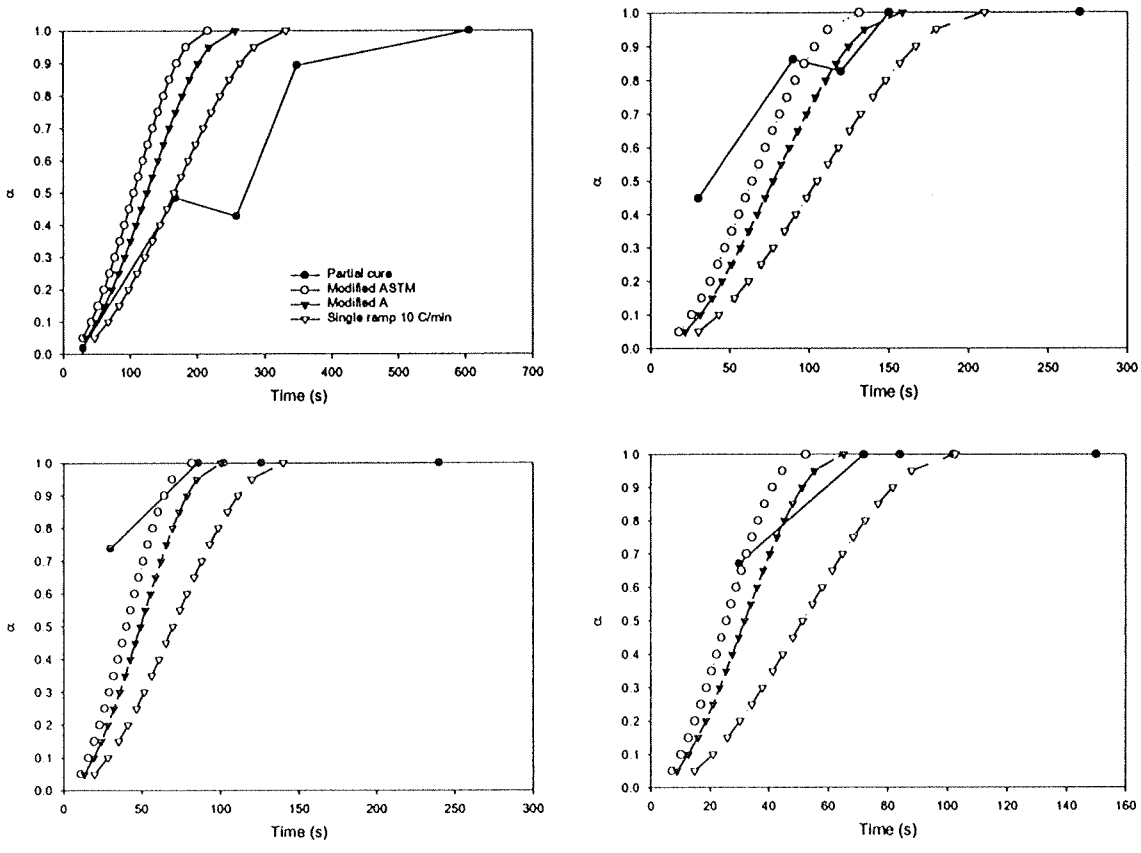

Fig. 6. Comparison of model cure predictions and partial cure DSC results for 110–140°C isotherms.

DSC and Fourier-transform infrared spectroscopy (FTIR) have been used to monitor the consumption of isocyanate during cure [1]. A large reduction in isocyanate peak height in the FTIR spectrum was observed prior to the onset of cure measured by μDEA for temperatures between 110 and 140°C. DSC partial cure experiments produced a similar reduction in heat generation above 120°C. Therefore, the majority of the heat generated during isothermal cure experiments conducted above 120°C was attributed to isocyanate consumption associated with increases in the molecular weight early in cure and not to crosslinking reactions that occur late in cure. Differences between single and multiple ramp DSC techniques for generating parameters are not obvious, since all DSC techniques should be insensitive to crosslinking reactions as demonstrated by partial cure studies. The majority of the cure for multiple ramps occurred in the region prior to 120°C with the exception of 15 and 20°C/min ramps (Table 2). The parameters calculated by the single ramp methods predicted the similar values despite the ramp rate.

A problem with the kinetic models generated by DSC and μDEA techniques is relating results to bond strength. A comparison between DSC and lap-shear data reveals a lag in bond development with respect to end of cure measured by DSC (Fig. 7). The lag becomes apparent in a comparison of model predictions from multiple ramps with lap-shear results. Bond strength still develops beyond the detectable levels of heat generation measured by partial cure studies at higher temperatures. Bond strength development at higher temperatures occurs through formation of a crosslinked network. μDEA techniques can accurately predict the point during cure of maximum shear strength because of its sensitivity to changes in morphology (Fig. 7). However μDEA measures a relative change in conductivity and cannot be related to the actual strength value.

5. Conclusions

Degree of cure and rate of cure calculated from μDEA data fit a first-order autocatalyzed kinetic model. The end of cure calculated by the μDEA models was earlier than that of the data. This difference maybe associated with the reaction being diffusion controlled and that the adhesive crystallizes late in cure. Activation energy and frequency factors for pMDI in a saturated steam environment as determined by μDEA were higher than those determined by calorimetric techniques. The higher activation energy could be associated with the formation of long polymer chains and crosslinked networks. Kinetic models developed from a single DSC temperature ramp consistently were similar to μDEA at high temperatures. Modified ASTM methods produce slightly higher activation energies, but the end of cure is predicted to be earlier. The end of cure for the modified ASTM methods corresponds closely to that observed earlier in partial cure study. All DSC methods produced activation energies lower than that of μDEA. This difference may indicate

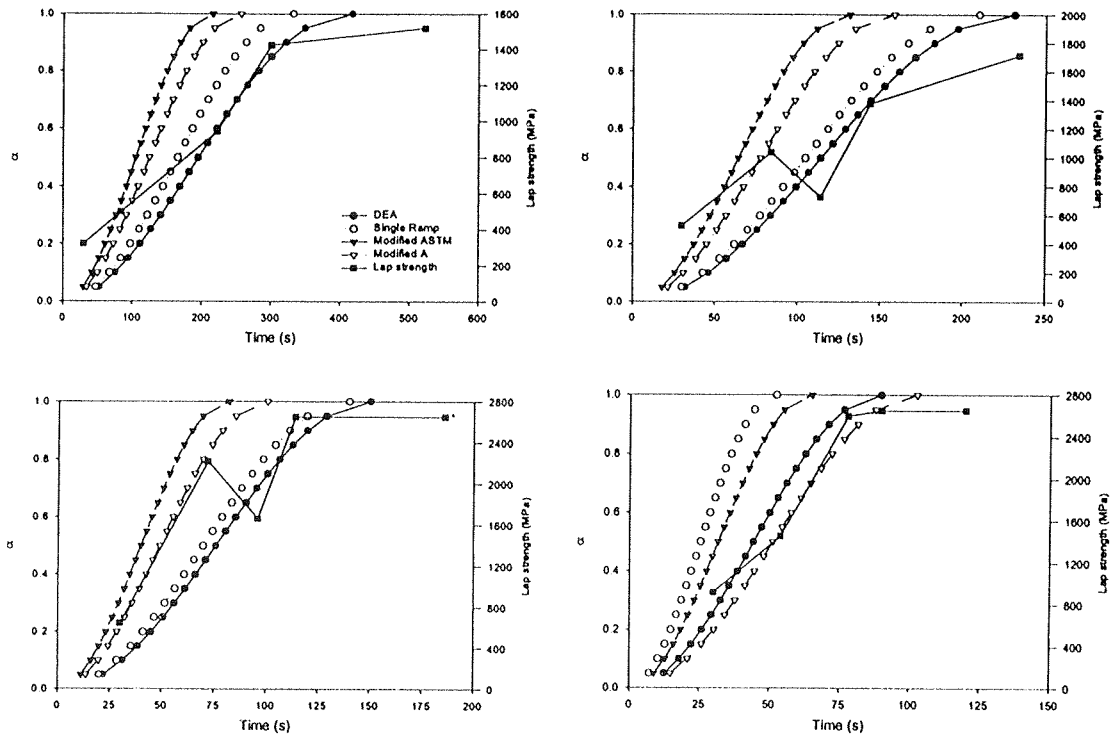

Fig. 7. Comparison of model degree of cure predictions and bond lap-shear strength for 110–140°C isotherms.

that DSC is more sensitive to the onset of cure where amine, urea, and urethane reactions could be taking place before network formation, and μDEA techniques are more sensitive to changes that occur in formation of a three-dimensional polymer network.

Acknowledgements

The authors would like to thank the USDA for their financial support and the staffs at the Southern Research Station in Pineville, LA and Wood Materials and Engineering Laboratory in Pullman, WA.

References

[1] Harper DP, Wolcott MP, Rials TG. J Adhesion, in press.
[2] Johns WE. Wood adhesives and technology. New York: Marcel Dekker Inc. 1983. p. 75–96.
[3] Weaver FW, Owen NL. Proceedings of Pacific Rim Bio-Based Composites Symposium, Rotorua, New Zealand, 1992. p. 143–153.
[4] Galbraith CJ, Newman WH. Proceedings of Pacific Rim Bio-Based Composites Symposium, Rotorua, New Zealand, November, 1992. p. 130–142.
[5] Wendler SL, Ni J, Frazier CE. Proceedings of Wood Adhesives 1995 Symposium, Madison, WI, 1995. p. 37–42.
[6] Rosthauser JW, Haider KW, Hunt RN, Gustavich WS. Proceedings of 30th International Particleboard/Composite Symposium, Pullman, WA, 1997. p. 161–75.
[7] Humphrey PE. Proceedings of Wood Adhesive in 1990: Status and Needs, Pullman, WA, 1990. p. 86–90.
[8] Geimer RL, Follensbee RA, Christiansen AW, Koutsky JA, Myers GE. Proceedings of Twenty-fourth International Particle board/Composite Symposium, Washington State University, Pullman, WA, 1990. p. 65–83.
[9] Humphrey PE, Zavala DJ. Test Eval 1989;17(6):323–8.
[10] Chelak W, Neman WH. Proceedings of Twenty-fifth International Particle board/Composite Symposium, Washington State University, Pullman, WA, 1990. p. 177–84.
[11] Wang X, Riedl B, Christiansen A, Geimer R. Polymer 1994;36(26):5685–92.
[12] Prime RB. Thermal characterization of polymeric materials. New York: Academic Press, 1981. p. 435–569.
[13] Provder T, Holsworth R, Grentzer T, Kline S. Advances in chemistry series polymer characterization: spectroscopic, chromatographic, and physical instrumental methods. Washington, DC: ACS, 1983. p. 233–53.
[14] Lam P. Polym Compos 1987;8(6):427–36.
[15] Annual Book of ASTM Standards. E698-79 Method. 1979; 14.02: 601.
[16] Doyle C. J Appl Polym Sci 1961;5(15):285–92.